

Stability Analysis for a Flexible Rotor on Active Magnetic Bearings subject to Aerodynamic Loads

Simon E. Mushi^{1,a}, Zongli Lin^{1,b}, Paul E. Allaire^{2,c}

¹Charles L. Brown Department of Electrical and Computer Engineering,
University of Virginia, Charlottesville, VA 22904-4743, U.S.A.

²Department of Mechanical and Aerospace Engineering,
University of Virginia, Charlottesville, VA 22904-4746, U.S.A.

{^asem5t, ^bzl5y, ^cpea}@virginia.edu

Abstract: The development of advanced control algorithms to guarantee stability and high performance of a rotor-AMB system subject to uncertainties and disturbances is an active area of research. The model based control paradigm entails consideration of the dynamics of all components that will affect the stability and performance of a system. Control design for a flexible rotor supported on active magnetic bearings provides an additional challenge since uncertainties such as the magnitudes of cross-coupled stiffness forces strongly affect the stability of the closed-loop system. Recent work has highlighted the use of sensitivity functions in determining stability margins for AMB supported turbomachinery. The output sensitivity function provides a means of quantifying the disturbance rejection and reference command tracking properties of the closed-loop system. Our work presents an analysis of the closedloop AMB sensitivity functions of the rotor-AMB system. We present simulations of the effects of varying mid-span aerodynamic cross-coupled stiffness on stability and performance of several μ -optimal controllers designed in a mixed-sensitivity framework, measurements of experimental sensitivity functions from the levitated rotor, and recommendations on the selection of weighting functions to improve the performance.

Keywords: Active Magnetic Bearing, Aerodynamic Cross-coupling, Mixed Sensitivity, Modeling and Identification, μ -synthesis, Robust Control

Introduction

Aerodynamic cross-coupled stiffness (CCS) forces in industrial compressors and turbines are a result of fluid-structure interactions produced by flow differences in clearances around impellers, seals, and hydrodynamic bearings. Observed early on in jet engines, the subsynchronous and self-exciting nature of these forces is of major concern to machinery designers as they create potentially unstable rotor vibrations, which can lead to machine damage in the absence of sufficient damping [1]. While empirical models exist for the factors that contribute to this aerodynamic CCS, the complex transient nature of the interactions makes it difficult to devise experiments and develop detailed design tools [2]. Several authors have described experiments in which active magnetic bearings (AMBs) have been used to excite a rotor-bearing system with CCS forces for various purposes [3,4,5].

In this work, we discuss and demonstrate the utility of sensitivity functions as a tool for design and analysis of controllers robust to varying levels of CCS. The use of the output sensitivity function as a tool to quantify the stability margins has been suggested in ISO

standard 14839-3 for AMB-supported turbomachinery [6], though it is not without some important limitations [7]. The recommendations within this standard have recently been used as part of a rotordynamic design audit tutorial using a 24.8MW AMB-supported pipeline compressor [8]. System sensitivity functions become a valuable asset in the design of control laws and respect the fundamental practical limitations on achievable stability and performance of rotor-AMB systems [9,10]. Recent works have continued to highlight the use of and investment in μ -synthesis control for AMBs as a powerful engineering tool to realize significant performance improvements over hand-tuned algorithms [11,12].

Test Rig Description

A rotor-AMB test rig (Fig. 1a) has been constructed at the University of Virginia to investigate the stability of AMB-supported turbomachinery subject to aerodynamic CCS forces and other uncertain aerodynamic loads [13]. The rotor has dimensions comparable to a small industrial centrifugal gas compressor such as the 25M frame size from Elliott's EDGE product line (6,600 to 21,200 m³/hr flow rate at 13,100 rpm with rotor length 1.145m to 2.285m). Our design consists of a 1.23m long steel rotor with a weight of 440 N and two gyroscopic disks. The average rotor diameter (excluding the attached components) is 60 mm. The larger disc weighs 82.8 N, has a diameter of 241.3 mm and imparts a significant gyroscopic character to the rotor. There are a total of four radial AMBs – two AMBs at the shaft ends to support the shaft with a combined load capacity of 2600N and two additional AMBs at the mid and quarter spans to allow for the application of simulated destabilizing fluid or electromagnetic forces to the rotor. All four AMBs operate with a 0.38mm air gap and a typical bias current of 2.95 A. The analog switching power amplifiers used to drive the AMBs operate from a 150V DC bus and have a maximum continuous current rating of 10A. Differential pairs of eddy current displacement sensors are used to determine the position of the rotor. The rotor can be driven up to 14,200 RPM using an AC motor and belt-drive system. A decentralized PID control algorithm is executed on a custom DSP platform at a 12 kHz sample rate for rotor levitation. Fig. 1b shows a schematic of the complete test rig.

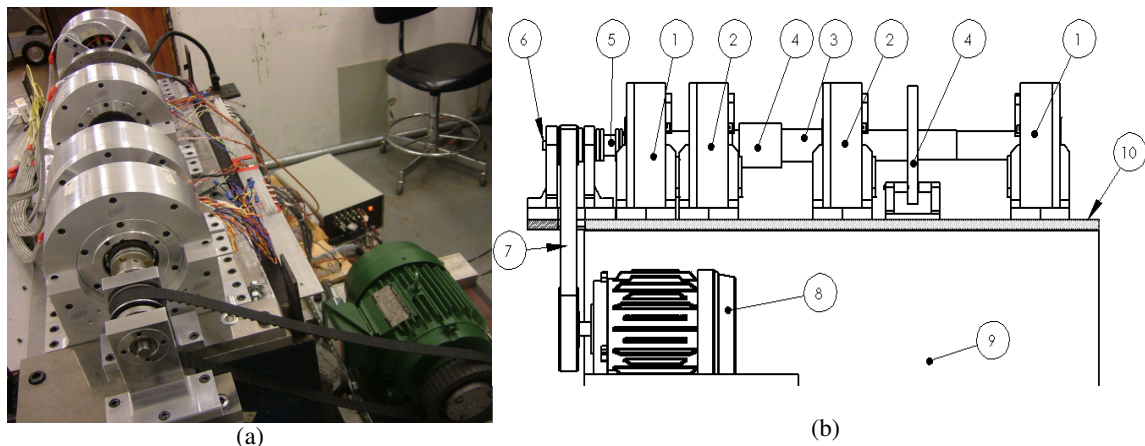


Figure 1: (a) Photograph of the test rig; (b) Schematic of test rig showing the major components :- (1) Support AMBs, (2) Exciter AMBs, (3) Rotor, (4) Gyroscopic discs, (5) Flexible coupling, (6) Jack shaft, (7) Timing belt, (8) 5 hp AC motor, (9) Concrete base, (10) Steel base.

Plant Modeling and Rotor Levitation

The modeling of high-speed rotor-AMB systems for control has been presented in the literature [5,10]. Typically a lateral rotordynamic analysis (undamped mode shapes and critical speed map) is performed using a finite-element rotor model as a starting point. Subsequently, the AMB properties can be analyzed using a magnetic reluctance circuit model to find a suitable bias current to perform bias flux linearization about. The resulting negative position stiffness K_x and current stiffness K_i can be used to approximate the AMB behavior when the rotor is within a neighborhood of the nominal air gap. Analytical models for the remaining electrical components and transducers (i.e., power amplifiers, position sensors, signal conditioning and data acquisition components) are appended to this model. See [14] for a detailed procedure for modeling high-speed rotor-AMB systems.

Following our rotordynamic analysis, the 49-station finite-element rotor model was modally reduced to retain two rigid body and three bending modes. Owing to the flexibility of the bearing pedestals, a foundation model with 6 modes was appended to the rotor model. The foundation model was identified experimentally and modal parameters were extracted using a grey-box iterative prediction error estimate approach [10]. This rotor-foundation model now has 44 first-order states describing the x and y motion at the two radial bearings. A linearized AMB actuator model with current gain, $K_i = 113.1$ N/A and negative position stiffness, $K_x = -0.967$ MN/m was then connected to the rotor-foundation model. The power amplifier in series with the AMB inductance was modeled with a 3rd order low pass filter with approximately 2.0 kHz small-signal bandwidth. The eddy current displacement sensors in series with an 8th order inverse Chebychev anti-aliasing filter demonstrated a flat magnitude response up-to 3 kHz, but contributed a significant phase lag of 40 degrees at 1 kHz. Lastly, a 2nd order Padé approximation for the 83.3 μ s controller computation delay (12 kHz sampling rate) was appended to the model. The plant model now contains 100 states, and compared well with the experimentally measured system (see Fig. 2).

The initial levitation of the rotor-AMB system at rest (0 RPM) is accomplished with a decentralized proportional-integral-derivative (PID) controller. The proportional gain ($K_p = 7.56$), integration time ($T_i = 0.075$) and derivative time ($T_d = 0.0023$) for each of the 4 control axes are obtained through experimental tuning. The basic PID controller is augmented with phase lead, notch filters and high-frequency roll-off to enable sufficient damping of the rotor bending modes within the controller bandwidth. The controller is able to levitate and center the rotor within 0.15s. The plant modeling and PID controller design are discussed extensively in our recent work [15].

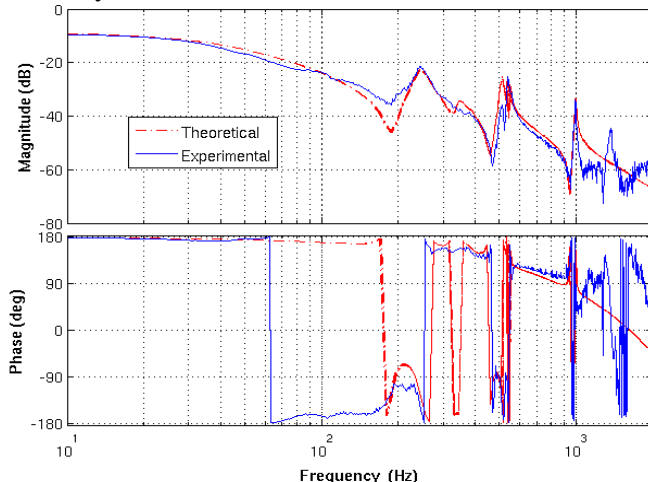


Figure 2: Bode plot from amplifier voltage input to sensor output showing dynamics of analytical rotor-AMB system theoretical model versus an experimental transfer function measurement for 1 axis.

Stability Margin Measurement

As mentioned earlier, ISO 14839-3 provides recommendations, based on experiment, for the evaluation of the stability margin for AMB-supported machinery, and makes important steps to bridge the communication gap between vendors, OEMs, and end-users of the equipment [6]. For newly commissioned machines, the standard suggests peak sensitivity less than 3 (in absolute terms or less than 9.5 dB), for a machine to be designated *Zone A*. Higher values of peak sensitivity values progressively decrease the classical closed-loop gain and phase margins and increase the likelihood of issues with a machine. *Zone B* is normally acceptable for unrestricted long-term operation with absolute peak sensitivity from 3 – 4; *Zone C* is unsatisfactory for long-term continuous operation with peak sensitivity from 4 – 5; and operation in *Zone D* is likely to cause machine damage with a peak sensitivity greater than 5. Fig. 3 shows an output sensitivity function for 2-axes of the rotor-AMB system measured at 0 RPM with an SR-785 dynamic system analyzer. The peak value above 8 indicates *Zone D* stability margin and it is likely that operation at design speed would cause machine damage. This peak corresponds to excitation of the 1st bending mode of the rotor and provides the engineer with an idea of where to place additional damping during controller tuning.

Limitations on the application of the output sensitivity function as a measure of stability margin were first mentioned in a paper by Li et al. [7]. The authors showed that with respect to destabilizing mechanisms such as cross-coupled stiffness, low peak sensitivities do not necessarily guarantee a good stability margin to this uncertainty, i.e., the measurements as proposed in ISO 14839-3 encompass a necessary but not sufficient condition for stability margin for multivariable systems. Therefore, to be more confident in stability margin assessment for certain machines, analysis of peak output sensitivity functions should be followed by an evaluation of the structured singular values, which gives an additional measure of robustness to specific uncertainties.

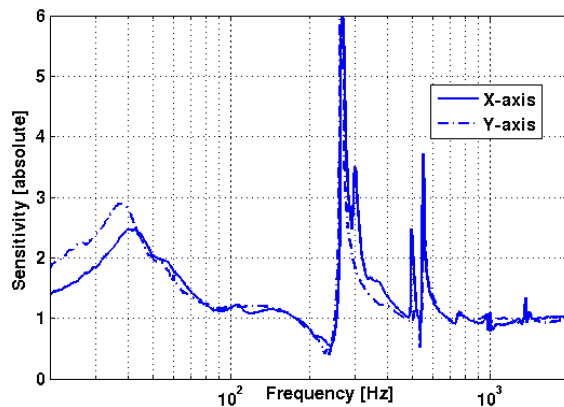


Figure 3: Experimental output sensitivity function at the non-driven end AMB while the rotor is levitated by a PID controller. A peak sensitivity value greater than 5 indicates a very poor stability margin.

Mixed-sensitivity and μ -optimal design

The goal of mixed-sensitivity control design is to optimize trade-offs among several system sensitivity functions to achieve the desired stability and performance specifications. The synthesis of controllers which minimize the H_∞ norm of the transfer function from disturbance input to performance output provides a means to attain desired performance specifications. However, such designs provide little guarantee of robustness with respect to uncertainties in plant parameters. The synthesis of μ -optimal controllers takes direct account of user-defined uncertainties during control design, and provides a guarantee in the form of the structured singular value for the amount of uncertainty the closed-loop system can

tolerate. For the sake of brevity, further discussion must be limited, however, the curious reader may find the following references insightful [16,17].

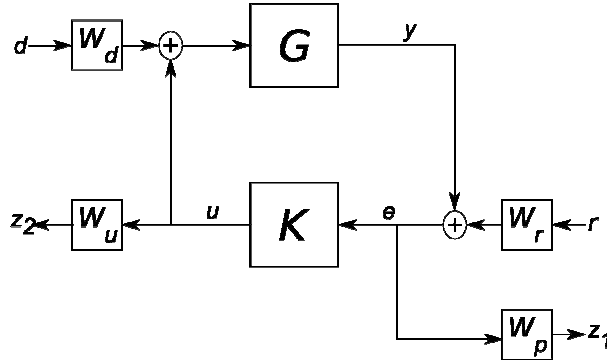


Figure 4: The “Gang of Four,” mixed-sensitivity framework block diagram. Input signals d and r are disturbance and reference inputs, respectively. Output signals z_1 and z_2 are actuator and position error performance signals, respectively.

The use of frequency-dependent weighting functions to capture the performance specifications for rotor-AMB systems is discussed extensively by several authors [9,10,11,12]. The four-block problem (see Fig. 4) uses the output sensitivity (S), process sensitivity (GS), control sensitivity (CS), and complementary output sensitivity (T) functions to form a performance constraint,

$$\left\| \begin{bmatrix} W_p S W_r & W_p G S W_d \\ W_u C S W_r & W_u T W_d \end{bmatrix} \right\|_{\infty} < 1, \quad (1)$$

where W_p is the performance specification weight, W_r is the reference input weight, W_d is the disturbance input weight, and W_u is the actuator dynamics weight. The selection of these frequency dependent weights is non-trivial and may be guided by insight into the system dynamics. A sub-optimal H_{∞} or μ -optimal controller, K , which stabilizes G (stability constraint) and also satisfies Eq. 1, will guarantee that $1/\|W_p W_d\|$ bounds GS , $1/\|W_p W_r\|$ bounds S , $1/\|W_u W_r\|$ bounds CS and $1/\|W_u W_d\|$ bounds T . For our control system the following weighting functions were adapted from [10],

$$W_p(s) = \frac{0.4s + \omega_I}{s + \beta\omega_I}, \quad W_u(s) = \frac{M_S}{M_{KS}} \frac{\omega_u^2 s^2 + 2\xi\omega_L + \omega_L^2}{\omega_L^2 s^2 + 2\xi\omega_u + \omega_u^2}, \quad W_d(s) = \frac{1}{M_{GS}}, \quad W_r = \frac{1}{M_S}, \quad (2)$$

where $M_S = 3$ enforces a bound on S , $M_{GS} = 0.085$ limits the peak value of T , $M_{CS} = 10/M_{GS}$, $\omega_B = 408\text{rad/s}$, $\omega_I = \omega_B/1500$ is the integrator time constant, $\omega_L = 10\omega_B$ defines the actuator bandwidth limitations, and ω_u is the frequency of complex poles inserted to ensure the reciprocal of W_u is proper. The resulting μ -optimal *Controller A* (designed without any CCS acting on the rotor) has a μ value of 0.856 and the peak output sensitivity over all four control axes is 2.29, indicative of an ISO *Zone A* stability margin. Compared with the PID controller in Fig. 3, the mixed-sensitivity optimization is able to improve damping of rotor and pedestal modes significantly. The only uncertainty considered in our plant model is the magnitude of the CCS force produced at the rotor mid-span. For the sake of brevity, the linear parameterization of this force used is

$$F_{xc} = -\chi \begin{bmatrix} 0 & 1 \\ -1 & 0 \end{bmatrix} \begin{bmatrix} q_{x\text{mid}} \\ q_{y\text{mid}} \end{bmatrix}, \quad (3)$$

where the scalar χ denotes the magnitude of the CCS force, and $q_{x\text{mid}}$ and $q_{y\text{mid}}$ are the

displacements at the rotor mid-span. We consider χ to be a real parametric uncertainty with values of 0 to 40,000 lbf/in (7 N/ μm) with a nominal value of 20,000 lbf/in (3.5 N/ μm). As we add 10,000 lbf/in and then 12,000 lbf/in of CCS to the rotor supported by *Controller A*, the peak sensitivity quickly rises through *Zone B* and *Zone C* at a frequency close to the conical rigid body mode (see Fig. 5a). As expected, the CCS generates a sub-synchronous excitation that eventually drives the system unstable. Another μ -optimal design *Controller B* was synthesized with a constant $\chi=20\,000\text{ lbf/in}$, while *Controller C* was synthesized with χ as an uncertain parameter over the range described earlier. All controllers have the same weighting matrices as defined in Eq. 2. Fig. 5b shows the effect of varying CCS on the simulated peak output sensitivity of the three controllers. As *Controller A* is optimized for zero cross coupled stiffness, it is able to guarantee a *Zone A* stability margin up to a 6,000 lbf/in of CCS. *Controller B* is able to guarantee *Zone A* stability margin from 13,500 – 26,000 lbf/in of CCS. At CCS values far from their design points both controllers *A* and *B*, are completely unable to stabilize the system. Interestingly, while *Controller C* was able to stabilize to system over the entire range of CCS, it can only guarantee a *Zone B* stability margin. The sub-optimal performance of *Controller C* may be improved by further tuning of the weighting functions to deal specifically with the low frequency sensitivity peak below 100 Hz caused by the CCS disturbance. By designing an online CCS estimator, it may also be possible to implement a gain scheduling approach to ensure stability and performance over a wider range of CCS as studied for changing running speed [10].

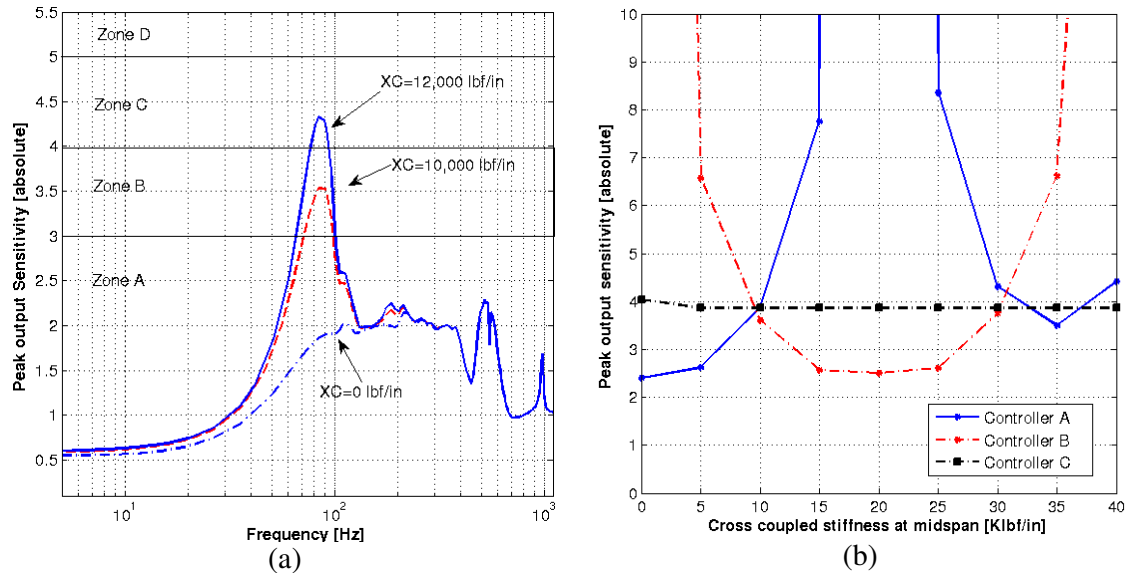


Fig. 5: (a) Peak sensitivity function for *Controller A* simulated with varying CCS, (b) Effect of CCS on peak output sensitivity functions of three μ -optimal controllers :- *A* designed for 0 lbf/in, *B* designed for 20 000 lbf/in, *C* designed for the entire range 0 – 40 000 lbf/in.

Conclusions

The use of sensitivity functions as a tool for the stability analysis and synthesis of control algorithms for rotor-AMB systems with uncertainties and disturbances has been evaluated using a mixed-sensitivity framework. The continued development and characterization of an AMB test rig with a flexible rotor allows us to evaluate the potential for model-based robust control design tools such as μ -synthesis to stabilize uncertain systems with practical

limitations such as actuator slew rate. Perhaps the greatest challenge in harnessing the power of mixed-sensitivity and μ -synthesis is the selection of weighting functions. However, as these functions take into account the properties and limitations of the control system their selection may be guided by engineering insight and thus tackled systematically. Further work on this project will involve practical generation of CCS forces using the mid-span AMB and the implementation of robust algorithms to stabilize the rotor-AMB system.

References

- [1] Alford, J., "Protecting turbomachinery from self-excited rotor whirl," *J. of Engineering for Power, Transactions of ASME*, Vol. 87(4) (1965), p. 333–344.
- [2] API 684, *API Standard Paragraphs Rotordynamic Tutorial*, 2nd edition, American Petroleum Institute, Washington D.C., U.S.A. (2005).
- [3] Ulbrich, H., "New test techniques using magnetic bearings," in *Proc. 1st Int. Symp. on Magnetic Bearings (ISMB-1)*, Zurich, Switzerland, (1988), p 281-288.
- [4] Cloud, H., *Stability of Rotors Supported by Tilting Pad Journal Bearings*, PhD dissertation, University of Virginia (2007).
- [5] Schweitzer, G., and Maslen, E.H., *Magnetic Bearings, Theory, Design, and Application to Rotating Machinery*, Springer-Verlag, Berlin, Germany (2009).
- [6] ISO 14839-3, Vibration of rotating machinery equipped with active magnetic bearings – Part 3: Evaluation of stability margin, International Standards Organization, (2006).
- [7] Li, G., Maslen, E., and Allaire, P., "A note on ISO AMB stability margin," in *Proc. 10th Int. Symp. on Magnetic Bearings (ISMB-10)*, Martigny, Switzerland, (2006), p.124-129
- [8] Swanson, E., Maslen, E., Li, G., and Cloud, C., "Rotordynamic design audit of AMB supported turbomachinery," *Proc. 37th Turbo. Symp.*, Houston, Texas, Sept. 8-11 (2008).
- [9] Schönhoff, U., *Practical Robust Control of Mechatronic Systems with Structural Flexibilities* PhD dissertation, Technical University of Darmstadt (2003).
- [10] Li, G., *Robust Stabilization of Rotor-Active Magnetic Bearing Systems*, PhD dissertation, University of Virginia (2006).
- [11] Maslen, E.H., and Sawicki, J.T., " μ -Synthesis for magnetic bearings: Why use such a complicated tool?," in *Proc. IMECE2007 ASME*, Seattle, U.S.A., Nov. 11-15 (2007).
- [12] Mystkowski, A., " μ -Synthesis control of flexible modes of AMB rotor," in *Proc. SMASIS2009 ASME*, Oxnard, CA, U.S.A., Sept. 21-23 (2009).
- [13] Mushi, S.E., *An Active Magnetic Bearing Test Rig for Aerodynamic Cross-coupling: Control Design and Implementation*, MS Thesis, University of Virginia (2008).
- [14] Li, G., Lin, Z., Allaire, P., and Luo, J., "Modeling of a high speed rotor test rig with active magnetic bearings," *J. Vibr. and Acoustics ASME*, Vol. 128(3) (2006), p. 269-281.
- [15] Mushi, S., Lin, Z., and Allaire, P., "Design, construction and modeling of a flexible rotor active magnetic bearing test rig," in *Proc. ASME Turbo Expo*, Glasgow, Scotland, June 14-18 (2010).
- [16] Sidi, M., *Design of Robust Control Systems: From Classical to Modern Practical Approaches*, Krieger Pub. Co., U.S.A., (2001).
- [17] Zhou, K., Doyle, J., and Glover, K., *Robust and Optimal Control*, Prentice Hall, Upper Saddle River, NJ, U.S.A, (1996).